

A Data-Driven Model for Anisotropic Heterogeneous Subsurface Scattering

Ying Song and Wencheng Wang

State Key Laboratory of Computer Science, Institute of Software, Chinese Academy of Sciences

E-mail: songy, whn@ios.ac.cn Tel: +86-10-62661652

Abstract—We present a new BSSRDF representation for editing measured anisotropic heterogeneous translucent materials, such as veined marble, jade, artificial stones with lighting-blocking discontinuities. Our work is inspired by the SubEdit representation introduced in [1]. Our main contribution is to improve the accuracy of the approximation while keeping it compact and efficient for editing. We decompose the local scattering profile into an isotropic term and an anisotropic term. The isotropic term encodes the scattering range and albedo property, and the anisotropic term encodes the spatial-variant subsurface scattering shape profile. We propose a compact model for the scattering profile based on non-negative matrix factorization, which allows user-guided editing. Experimental results have shown that our model can capture more spatial-anisotropic features than the previous work with similar compression rate.

I. INTRODUCTION

The subsurface scattering of light is known for its distinctive impact on the realistic visual appearance, as well as the challenge for accurate and efficient rendering or editing. For heterogeneous materials, the appearance is determined by the complex light interactions with the constituents elements inside the volume, which have different optical properties and uneven spatial distributions. *Volume-based* approach[2–4] constructs a volume with spatial-varied scattering properties and simulates light transport inside the volume. Although some can induce the scattering properties from real world samples and achieve interactive rates [2, 3], it is not effective to get a specific result by directly editing the properties.

An alternative *Surface-based* approach uses bidirectional subsurface scattering reflectance distribution function(BSSRDF) [5] to model the subsurface scattering. Generally, the BSSRDF encodes the light transport within the volume by recording the relationship between each pair of incoming and outgoing surface points. For homogeneous materials, analytic models[6, 7] can be used to approximate the subsurface scattering by which several editing methods are inspired [2, 8]. The homogeneous scattering properties can also be measured by fitting to the analytic model from real world image samples [6, 9]. However, these methods are not suitable for heterogeneous materials. Several data-driven methods [10–12] are accomplished to recover the appearance of a translucent object from images samples with dense measurement or sampling, but none of them consider modifying it explicitly. SubEdit system [1] decouples a measured BSSRDF into products of two separate radial-core profiles of entry and exit points. Each profile of a surface point can

be further parameterized into the several appearance concepts to facilitate intuitive editing. However, this method is less suited for representing anisotropic scattering behavior due to the radial nature of the profile. For instance, materials such as veined marble, jade, or artificial stones always exhibit strong anisotropic scattering behavior. Our model is inspired by their method. The key to our representation is the compact factorized shape profile instead of the one-dimensional radial function. The scattering behavior at a single surface location can be accurately approximated by two factored vectors, even for highly anisotropic materials. Based on this representation, extended editing operations for anisotropy can be developed to provide more options to edit the visual appearance of the subsurface scattering material. Some image-based editing operations can be borrowed into the editing because the result of the factorization can be reorganized as shape profile textures. Furthermore, this new representation can be incorporated into existing hierarchical[13] or multi-resolution GPU-accelerated visualization systems [14] and get high quality anisotropic non-local subsurface scattering effects (Fig. 1).

To summarize, this paper presents a new representation for real world anisotropic heterogeneous materials, which has the following distinctive features:

- **Accuracy.** It accurately fits highly anisotropic measured data while maintaining the independence of the scattering profile.
- **Compactness.** It is compact and potentially allows interactive editing and rendering.
- **Extensive editing operations.** It explores novel editing possibilities on anisotropy and heterogeneity.

II. RELATED WORKS

Early research on the representation of a BSSRDF mainly focus on realistic appearance or fast simulation. The modification of the BSSRDFs is an emerging requirement over the past a few years. Recent works on BSSRDF representation can be roughly categorized into analytic models and data-driven models. To avoid the full complexity of the light transport, both categories of models need certain levels of approximation.

A. Analytic Models

Analytic models use physical scattering parameters to represent the translucent material. Homogeneous materials usually apply analytic models because the scattering parameters are uniform. A successful approach is the dipole approximation

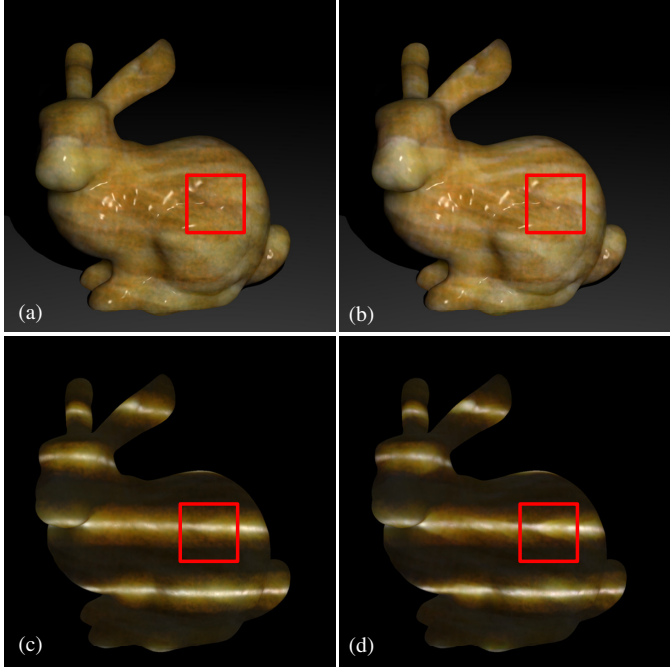


Fig. 1. A measured jade material applied to Stanford Bunny using SubEdit and our representation. (a) Rendering with SubEdit representation. (b) Rendering with our representation. The anisotropy causes more contrast in details. (c) SubEdit under strip pattern lighting. (d) Our representation under strip pattern lighting. Our representation exhibits more anisotropic features as shown in red box regions.

model[6] which enables fast visualization. It also provides the method to measure the scattering parameters of planar material samples. Based on the dipole model, Munoz et al.[9] propose a method to acquire the parameters from a single image. The dipole model also inspires several editing methods [8] [15] for homogeneous materials by changing the combination of several basis profiles. A multi-layered analytic model[7] is derived from the dipole model to describe heterogeneous materials with homogeneous layers. François et al.[16] applied 2D thickness textures to describe the multi-layered model and achieved realtime rendering.

For heterogeneous, optically dense materials, the scattering parameters cannot be directly retrieved or edited based on above methods. Wang et al.[2] use the diffusion equation to model subsurface scattering, and present a GPU implementation fast enough to be used for realtime editing of the material properties, which is later extended to tetrahedral meshes [3]. An inverse solver is also proposed to extract the scattering properties from measured heterogeneous scattering materials. However, mapping from editing operations to the appearance is not clear in their work. Hašan et al.[4] manage to edit the local albedo coefficients by precomputing the albedo-intensity and albedo-pixel mapping in a path-tracing system. They extend the diffusion assumption to a more general case of physical simulation, while in the cost of limited editing options. Our approach followed the diffusion assumption, allowing the user to directly control the appearance properties of

the scattering material: albedo, scattering range, and scattering profile.

B. Data-driven Models

Several methods compute spatially varying scattering properties by fitting the dipole model to BSSRDFs at each point[7, 17] or per region[18, 19]. However, these methods can only represent materials with slowly varying properties such as skin. They cannot handle heterogeneous translucent materials with sharp variations, such as marble and jade. Goesele et al.[11] capture the subsurface properties for specific geometry, where neither material nor geometry can be modified. Peers et al. [10] factorize spatial variations in terms of incident and outgoing locations via a modified non-negative matrix factorization. Their representation is compact, but cannot be edited directly. Song et al.[1] introduce SubEdit system for editing measured BSSRDF for the first time. However, SubEdit gets relative high error for spatial anisotropic heterogeneous materials. Under the observation that by eliminating the isotropic effect from the scattering profile, factorization tool can be suitable for highly anisotropic data, our work decomposed the local scattering profile into an isotropic and an anisotropic term. The isotropic term accounts for the homogeneous scattering behavior, while the anisotropic term accounts for the spatially anisotropic subsurface scattering.

C. BRDF Editing

Interactive editing of BRDFs is possible for analytic BRDF models by directly manipulating the parameters or by artist-friendly interface[20]. For data-driven BRDF editing involved with large datasets, factorization tools are popular to facilitate global illumination and material changing [21, 22]. Those methods are designed for BRDF or BTF and has no spatial component. Lawrence et al. [23] use constrained matrix factorization to represent and edit spatially varying BRDFs, assuming that the BRDF is a separable function. It is not clear how to extend these techniques to BSSRDF.

III. REPRESENTATION

A. Preliminaries

Diffuse BSSRDF. In this paper we applied the diffuse BSSRDF $S_d(\mathbf{x}_i, \omega_i, \mathbf{x}_o, \omega_o)$ as a simplification of the full BSSRDF $S(\mathbf{x}_i, \mathbf{x}_o, \omega_i, \omega_o)$ [5] to avoid the tremendous storage of data acquisition and complexity of rendering. The diffuse BSSRDF describes the behavior of subsurface scattering materials by relating the outgoing radiance $L(\mathbf{x}_o, \omega_o)$ at a point \mathbf{x}_o in direction ω_o to the incoming radiance $L(\mathbf{x}_i, \omega_i)$ at a location \mathbf{x}_i and incoming direction ω_i as:

$$L(\mathbf{x}_o, \omega_o) = \int_A \int_{\Omega} S_d(\mathbf{x}_i, \omega_i, \mathbf{x}_o, \omega_o) L(\mathbf{x}_i, \omega_i) (n(\mathbf{x}_i) \cdot \omega_i) d\omega_i d\mathbf{x}_i \quad (1)$$

where A is the surface area, Ω is the upper hemisphere around \mathbf{x}_i , and $n(\mathbf{x}_i)$ is the surface normal at \mathbf{x}_i . The diffuse BSSRDF can be further decomposed as

$$S_d(\mathbf{x}_i, \omega_i, \mathbf{x}_o, \omega_o) = \frac{1}{\pi} F_i(\mathbf{x}_i, \omega_i) R_d(\mathbf{x}_i, \mathbf{x}_o) F_o(\mathbf{x}_o, \omega_o),$$

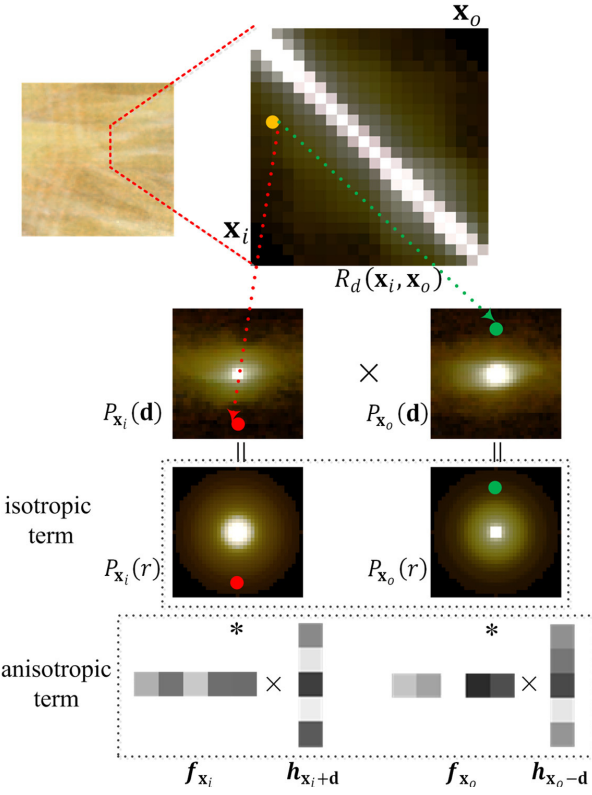


Fig. 2. Overview of our representation. The subsurface transport R_d from a single entry to exit point (marked in yellow) is expressed as the product of corresponding points in the factored scattering profiles at \mathbf{x}_i (marked in red) and at \mathbf{x}_o (marked in green). The scattering profile is further decomposed into an isotropic term and an anisotropic term. The anisotropic term is represented by matrix factorization.

where F_o and F_i are Fresnel transmission coefficients, and R_d is a four dimensional function of two surface locations that encodes the spatial subsurface scattering of heterogeneous materials. Following previous work [1, 10, 11], we eliminate the angular influence of the measured material.

Data Acquisition. We expect the acquired BSSRDF data to be applied to any geometry at the cost of additional computations or approximations. In this paper, we adopted the approach in Ref. [10] for capturing the diffuse BSSRDF from planar material samples.

B. Anisotropic Representation

In SubEdit representation, the non-local scattering behavior of the BSSRDF is decoupled into per-point local scattering profiles:

$$R_d(\mathbf{x}_i, \mathbf{x}_o) = \sqrt{P_{\mathbf{x}_i}(r)P_{\mathbf{x}_o}(r)},$$

where $P_x(r)$ is an isotropic 1D radial function around a surface, and $r = \|\mathbf{x}_o - \mathbf{x}_i\|$. Although this approximation can represent a variety of measured materials, it cannot accurately reproduce strong anisotropic scattering caused by narrow discontinuities in the material volume like marble veins. A straightforward solution is to extend the 1D radial function to

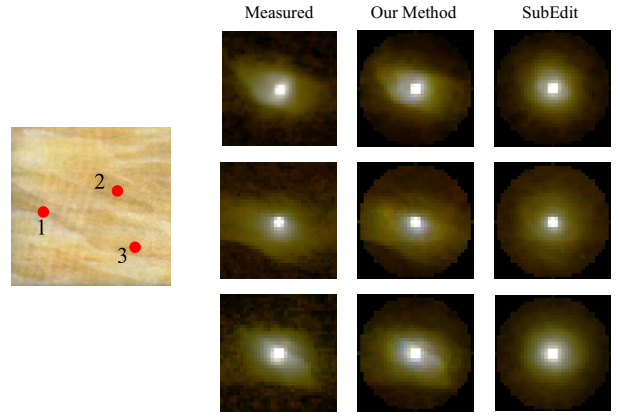


Fig. 3. The measured BSSRDFs, reconstructed BSSRDFs by our method and SubEdit method from three locations of a measured chessboard sample (left). The first row to the third row corresponds to point 1-3.

2D as:

$$R_d(\mathbf{x}_i, \mathbf{x}_o) = \sqrt{P_{\mathbf{x}_i}(\mathbf{d})P_{\mathbf{x}_o}(-\mathbf{d})},$$

where $\mathbf{d} = \mathbf{x}_o - \mathbf{x}_i$, indicating the scattering direction over a near-planar surface around \mathbf{x} . Accuracy is guaranteed thanks to the 2D scattering profile, which also leads to the same amount of storage as the diffuse BSSRDF R_d . In order to find a suitable factored form to represent the 2D scattering profile $P_x(\mathbf{d})$, we first sample \mathbf{d} over the whole plane the same dimension as R_d and store $P_x(\mathbf{d})$ in a matrix $P(\mathbf{x}, \mathbf{x} + \mathbf{d})$. By dividing out the isotropic term, we further factor the residue into a feature matrix $F(\mathbf{x}, t)$ and coefficient matrix $H(t, \mathbf{x} + \mathbf{d})$:

$$P(\mathbf{x}, \mathbf{x} + \mathbf{d}) \approx G(\mathbf{x}, \mathbf{x} + \mathbf{d}) * (F(\mathbf{x}, t)H(t, \mathbf{x} + \mathbf{d})), \quad (2)$$

where G is the isotropic term matrix constructed from $P_x(r)$, and $*$ indicates component-wise matrix multiplication. The user-defined term t (width of F and height of H) determine the degree of approximation of the scattering profile. Note that the isotropic term matrix only need minimal storage as $P_x(r)$. If we denote the row vector of F as \mathbf{f}_x , and the column vector of H as \mathbf{h}_x , the scattering profile on a location \mathbf{x} can be approximated as:

$$P_x(\mathbf{d}) \approx P_x(r)(\mathbf{f}_x \cdot \mathbf{h}_{\mathbf{x}+\mathbf{d}}), \quad (3)$$

As visualized in Fig. 2, the isotropic term $P_x(r)$ encodes the homogeneous scattering behavior, which is the combination of diffuse albedo and average scattering range. The anisotropic term encodes the local spatial-varied scattering patterns which are obtained by matrix factorization. The subsurface scattering from a single entry to an exit point is expressed as the product of corresponding points in the scattering profile at the two locations.

Fig. 3 compares the BSSRDFs reconstructed from SubEdit and our method. Notice that our method performs better in most of the anisotropic case. The comparison of rendering the geometry is shown in Fig. 1.

C. Factorization

The diffuse BSSRDF $R_d(\mathbf{x}_i, \mathbf{x}_o)$ and the scattering profile $P_{\mathbf{x}}(\mathbf{d})$ on a surface point \mathbf{x} can both be regarded as linearized vectors of surface points within the scattering range. Before factorization, we should fit the 2D scattering profile first. Ideally the diffuse BSSRDF matrix would be symmetric, but measured data does not keep the rule due to measurement error. We enforce the symmetry by averaging the reverse response. The 2D scattering profile is initialized according to the symmetric diffuse BSSRDF matrix. We used non-negative matrix factorization (NMF) [24] to lower the dimension of the scattering shape matrix. Because the result of the calculation remains positive, the non-negative terms enable importance sampling and further editing. We adopted the updating rules in [10] to factor out the matrix:

$$H \leftarrow H * \left(F^T \frac{\max(P - c_{sparse}, \varepsilon)}{(FH) * G + \varepsilon} \right),$$

$$F \leftarrow F * \left(\frac{\max(P - c_{sparse}, \varepsilon)}{(FH) * G + \varepsilon} H^T \right),$$

In each iteration, we normalized the column vector to provide desired sparseness. A small ε is added to the denominator to avoid dividing by zero. A sparseness parameter c_{sparse} can also be added to the update rule to provide sparseness of the feature images. In experiment, ε was set to $1e-16$ and c_{sparse} was set from 0.01 to 0.2.

Theoretically, the BSSRDF should preserve three following basic principles of physics during modifying or rendering, as the case of BRDF editing in [25], reciprocity, non-negativity and energy conservation. Our representation fulfills the reciprocity automatically. The non-negativity is also preserved by the non-negative matrix factorization method. Energy conservation is easy to preserve if we enforce this after each editing operation is performed.

IV. EDITING

In this work we perform the editing operations on the plane sample and map the material onto objects. In order to edit the scattering profile $P_{\mathbf{x}}$ in a more intuitive way, we reparameterize the 2D scattering profile into three independent terms: its diffuse albedo $A_{\mathbf{x}}$, the scattering range $\mu_{\mathbf{x}}$, and the 2D scattering shape profile $S_{\mathbf{x}}(\mathbf{d})$:

$$P_{\mathbf{x}}(\mathbf{d}) = \frac{A_{\mathbf{x}}}{\mu_{\mathbf{x}}^2} G_{\mathbf{x}}\left(\frac{r}{\mu_{\mathbf{x}}}\right) S_{\mathbf{x}}\left(\frac{\mathbf{d}}{\mu_{\mathbf{x}}}\right), \quad (4)$$

Assuming s and t as the two dimensions of \mathbf{d} , the diffuse albedo $A_{\mathbf{x}} = \int \int P_{\mathbf{x}}(s, t) ds dt$ captures the diffuse reflectance of location \mathbf{x} . The scattering range $\mu_{\mathbf{x}}$ indicates the maximum scattering radius of the surface point. The scattering shape profile $S_{\mathbf{x}}(\mathbf{d})$ implicates the anisotropic scattering behavior of the material. We do not manipulate the scattering shape profile directly. Instead, the factored matrix F and H can be reorganized as feature and coefficient images to describe the scattering pattern of the material. An example of part of the Jade material is presented in Fig. 4.

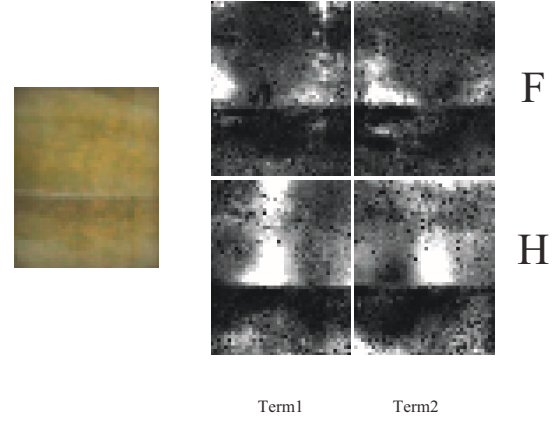


Fig. 4. The visualized feature image and coefficient image of NMF. Note How the F and H images captures the light-blocking feature of the material.

Modifying the NMF textures directly with image editing algorithms like filtering, edge enhancing, etc, would provide extensive editing operations to the BSSRDF data. For instance, add a sudden drop in the feature texture would cause a light-blocking effect on the material. To conserve the energy, we make sure $S_{\mathbf{x}}$ to be normalized after each editing operation.

Since the editing of BSSRDF material is a non-local operation, we need to define the appearance metrics to perform the soft selection and editing propagation. The distance between two surface point \mathbf{x} and \mathbf{y} is defined as:

$$d^2(\mathbf{x}, \mathbf{y}) = \int_0^\infty \|G_{\mathbf{x}}(r) - G_{\mathbf{y}}(r)\|^2 r dr + \alpha \sum_{i=0}^t \|F(\mathbf{x}, i) - F(\mathbf{y}, i)\|^2 + \beta \sum_{i=0}^t \|H(i, \mathbf{x}) - H(i, \mathbf{y})\|^2, \quad (5)$$

where α and β are user-specified weight to measure the anisotropy difference. In experiments, we set $\alpha = 1.0$ and $\beta = 1.0$. After selection, the altered parameters needs to be propagated to other surface points by linear interpolation with the normalized difference as the scaling weight. We show some editing results in Fig. 5 by modifying the three scattering parameters separately.

V. RESULTS AND DISCUSSION

In this paper, all results were produced on a PC with Intel Core 2 Dual 3.20GHz CPU with 6GB RAM and an NVIDIA GTX 480 graphics card with 1.6GB video memory. All images were rendered with our interactive renderer at 3-5 frames per second.

Table I lists the compression performance of the measured BSSRDF datasets. We sampled the measured data with 8 non-uniform segments for $P(r)$, based on the fact that further scattering response needs less samples to fit because of the multiple scattering effect. After fitting the isotropic term, we factored the scattering shape profile using NMF. We measured the quality of the fit by computing the minimum, average

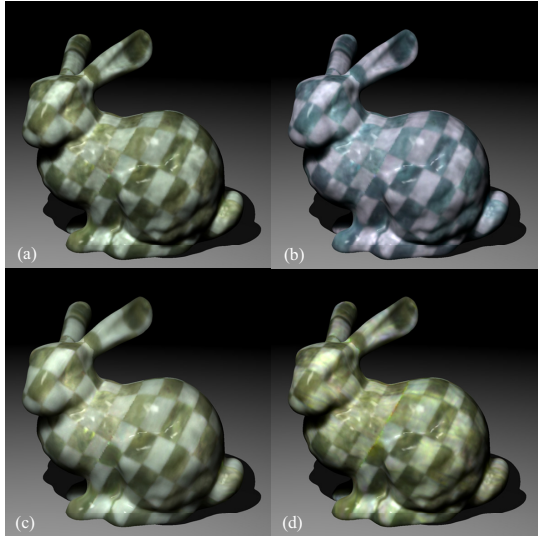


Fig. 5. Editing results of the Chessboard marble material. (a) Original. (b) Altering the albedo value. (c) Increasing the scattering range. (d) Migrating the F and H texture from the Jade material to the chess material.

TABLE I
COMPRESSION RESULT

Sample Material	Res. (pixels)	Terms	Orig. Size	Fact. Size	Min/Avg/Max Relative Error
Chessboard	222x222	10	674M	18.2M	0.019/0.06/0.117
Artif. Stone	108x108	16	163M	6.9M	0.002/0.008/0.10
Jade	260x260	20	947M	37.3M	0.001/0.01/0.062

and maximum of the relative errors at each surface location between the measured data and the reconstructed data normalized by the total energy of the response, as in [1]. Although our data size is slightly larger than previous work, we can perform consistent editing operations and represent accurate anisotropic subsurface scattering.

We implemented a GPU-accelerated renderer to interactively visualize the rendering and edited results in this paper. The majority of the computation is the integrals over the surface according to 1. We used the two-pass method of Jensen and Buhler[26] to evaluate the final radiance. In the first pass, we built the irradiance map for each mesh vertex using shadow map based method for local illumination, or from precomputed radiance transfer techniques for global illumination[27]. In the second pass, we integrated the contributions from neighborhood surface samples for each vertex to compute the outgoing radiance. An octree hierarchy on a GPU is used to accelerate the rendering phase[13]. The visiting of neighboring vertices was parallelized on a GPU using CUDA. Since it is a vertex-based algorithm, the mesh should be sufficiently tessellated to obtain visual plausible result.

We have applied our representation on several measured materials with anisotropic subsurface scattering. All the results are shown in simple lighting, which is not limited to. In Fig. 6 the measured chessboard material was mapped to the Stanford Dragon model. Our parameterization allows us to linearly

interpolate all the components for edits, so it is possible to transfer the scattering behavior between different materials. First we increased the scattering range of the chess board material, then we transferred the scattering shape profile from the jade material. Note that the scattering behavior changes in the geometry details in Fig 6(c). Fig. 7 shows the result of changing anisotropy by directly enhancing or filtering the scattering feature matrix. Fig. 8 shows the rendering result of another measured material mapped on the bird model with thin parts.

VI. CONCLUSIONS AND FUTURE WORK

In this paper we presented a compact representation for editing measured spatial-anisotropic heterogeneous subsurface scattering. The non-local scattering properties are decomposed as isotropic and anisotropic terms. Non-negative matrix factorization was applied to the anisotropic term, while the global term is represented by the parameters that directly map to appearance concepts. This decoupling allows users to directly modify the scattering of single surface locations and makes editing extensible to the local anisotropy.

In the future we are interested in exploring different clustering method other than NMF to better interpreting the subsurface scattering dataset. Despite the efficient rendering and basic editing operations, we are looking forward to exploring more advanced editing operations based on feature textures. Finally, we are interested in exploring rendering algorithms to employ the editing directly on mesh and bring more practical applications.

VII. ACKNOWLEDGMENT

The authors would like to thank Xin Tong for providing the measured BSSRDF data. This work was partially supported by the national natural science foundation of China (Proj. number: 61379087).

REFERENCES

- [1] Y. Song, X. Tong, F. Pellacini, and P. Peers, “Subedit: a representation for editing measured heterogeneous subsurface scattering,” *ACM Trans. Graph.*, vol. 28, pp. 31:1–31:10, July 2009.
- [2] J. Wang, S. Zhao, X. Tong, S. Lin, Z. Lin, Y. Dong, B. Guo, and H.-Y. Shum, “Modeling and rendering of heterogeneous translucent materials using the diffusion equation,” *ACM Trans. Graph.*, vol. 27, pp. 9:1–9:18, Mar. 2008.
- [3] Y. Wang, J. Wang, N. Holzschuch, K. Subr, J.-H. Yong, and B. Guo, “Real-time rendering of heterogeneous translucent objects with arbitrary shapes,” *Computer Graphics Forum*, vol. 29, April 2010.
- [4] M. Hašan and R. Ramamoorthi, “Interactive albedo editing in path-traced volumetric materials,” *ACM Trans. Graph.*, vol. 32, pp. 11:1–11:11, Apr. 2013.
- [5] F. E. Nicodemus, J. C. Richmond, J. J. Hsia, I. W. Ginsberg, and T. Limperis, “Radiometry,” ch. Geometrical

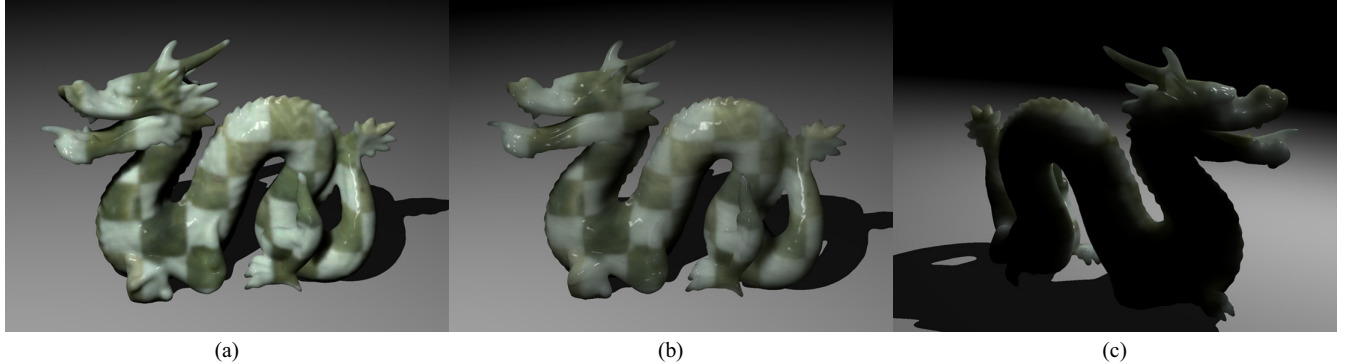


Fig. 6. Measured chessboard marble BSSRDF mapped on the Stanford Dragon model. (a) the rendering result of the original material in simple lighting. (b) The scattering feature of the Jade material is transferred to the chessboard marble and the scattering range is increased. (c) The back lighting effect to show the heterogeneity.

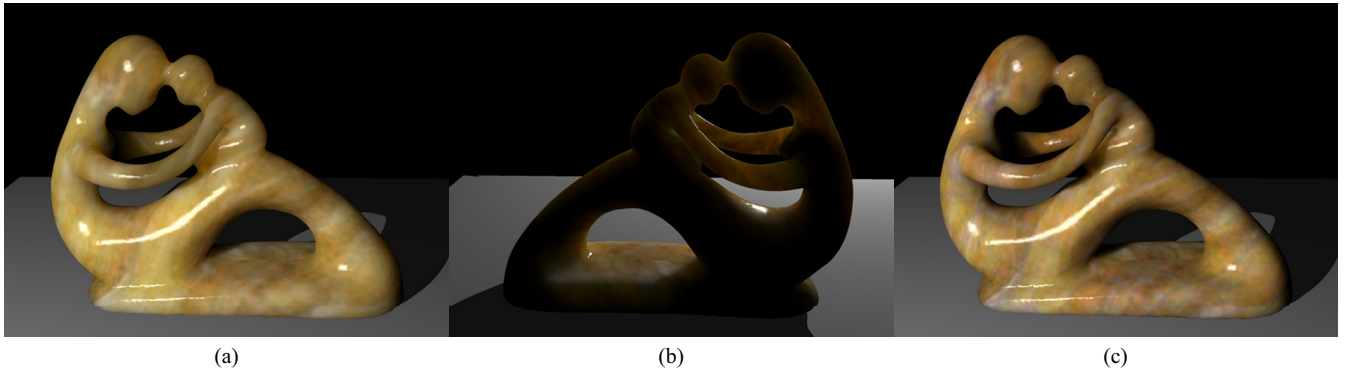


Fig. 7. Measured Jade BSSRDF mapped on the sculpture model. (a)Original material. (b) Back-lighting. (c)Enhanced anisotropy by filtering the F and H images.

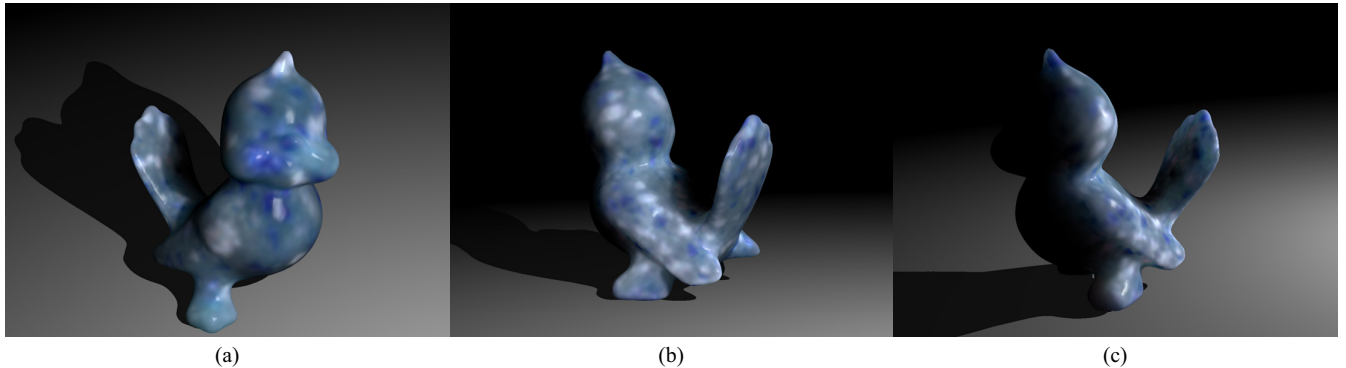


Fig. 8. Measured artificial stone BSSRDF mapped on the bird model in different views.

considerations and nomenclature for reflectance, pp. 94–145, USA: Jones and Bartlett Publishers, Inc., 1992.

- [6] H. W. Jensen, S. R. Marschner, M. Levoy, and P. Hanrahan, “A practical model for subsurface light transport,” in *Proceedings of the 28th annual conference on Computer graphics and interactive techniques*, SIGGRAPH ’01, (New York, NY, USA), pp. 511–518, ACM, 2001.
- [7] C. Donner, T. Weyrich, E. d’Eon, R. Ramamoorthi, and S. Rusinkiewicz, “A layered, heterogeneous reflectance model for acquiring and rendering human skin,” *ACM*

Trans. Graph., vol. 27, pp. 140:1–140:12, Dec. 2008.

- [8] K. Xu, Y. Gao, Y. Li, T. Ju, and S.-M. Hu, “Real-time homogenous translucent material editing,” *Comput. Graph. Forum*, vol. 26, no. 3, pp. 545–552, 2007.
- [9] A. Munoz, J. I. Echevarria, F. Seron, J. Lopez-Moreno, M. Glencross, and D. Gutierrez, “BSSRDF estimation from single images,” *Computer Graphics Forum*, vol. 30, pp. 455–464, 2011.
- [10] P. Peers, K. vom Berge, W. Matusik, R. Ramamoorthi, J. Lawrence, S. Rusinkiewicz, and P. Dutré, “A compact

- factored representation of heterogeneous subsurface scattering,” *ACM Trans. Graph.*, vol. 25, pp. 746–753, July 2006.
- [11] M. Goesele, H. P. A. Lensch, J. Lang, C. Fuchs, and H.-P. Seidel, “Disco: acquisition of translucent objects,” *ACM Trans. Graph.*, vol. 23, pp. 835–844, Aug. 2004.
- [12] X. Tong, J. Wang, S. Lin, B. Guo, and H.-Y. Shum, “Modeling and rendering of quasi-homogeneous materials,” *ACM Trans. Graph.*, vol. 24, pp. 1054–1061, July 2005.
- [13] K. Zhou, M. Gong, X. Huang, and B. Guo, “Data-parallel octrees for surface reconstruction,” *IEEE Transactions on Visualization and Computer Graphics*, vol. 17, pp. 669–681, May 2011.
- [14] G. Chen, P. Peers, J. Zhang, and X. Tong, “Real-time rendering of deformable heterogeneous translucent objects using multiresolution splatting,” *Vis. Comput.*, vol. 28, pp. 701–711, June 2012.
- [15] R. Wang-erb, E. Cheslack-Postava, R. Wang, D. Luebke, Q. Chen, W. Hua, Q. Peng, and H. Bao, “Real-time editing and relighting of homogeneous translucent materials,” *Vis. Comput.*, vol. 24, pp. 565–575, July 2008.
- [16] G. Fran ois, S. Pattanaik, K. Bouatouch, and G. Breton, “Subsurface texture mapping,” *IEEE Computer Graphics and Applications*, vol. 28, no. 1, pp. 34–42, 2008.
- [17] S. Tariq, A. Gardner, I. Llamas, A. Jones, P. Debevec, and G. Turk, “Efficient estimation of spatially varying subsurface scattering parameters,” in *11th International Fall Workshop on Vision, Modeling and Visualization*, (Aachen, Germany), June 2006.
- [18] T. Weyrich, W. Matusik, H. Pfister, B. Bickel, C. Donner, C. Tu, J. McAndless, J. Lee, A. Ngan, H. W. Jensen, and M. Gross, “Analysis of human faces using a measurement-based skin reflectance model,” *ACM Trans. Graph.*, vol. 25, pp. 1013–1024, July 2006.
- [19] A. Ghosh, T. Hawkins, P. Peers, S. Frederiksen, and P. Debevec, “Practical modeling and acquisition of layered facial reflectance,” *ACM Trans. Graph.*, vol. 27, pp. 139:1–139:10, Dec. 2008.
- [20] M. Colbert, S. Pattanaik, and J. Krivanek, “Brdf-shop: Creating physically correct bidirectional reflectance distribution functions,” *IEEE Comput. Graph. Appl.*, vol. 26, pp. 30–36, Jan. 2006.
- [21] A. Ben-Artzi, K. Egan, F. Durand, and R. Ramamoorthi, “A precomputed polynomial representation for interactive brdf editing with global illumination,” *ACM Trans. Graph.*, vol. 27, pp. 13:1–13:13, May 2008.
- [22] X. Sun, K. Zhou, Y. Chen, S. Lin, J. Shi, and B. Guo, “Interactive relighting with dynamic brdfs,” *ACM Trans. Graph.*, vol. 26, July 2007.
- [23] J. Lawrence, A. Ben-Artzi, C. DeCoro, W. Matusik, H. Pfister, R. Ramamoorthi, and S. Rusinkiewicz, “Inverse shade trees for non-parametric material representation and editing,” *ACM Trans. Graph.*, vol. 25, pp. 735–745, July 2006.
- [24] D. D. Lee and H. S. Seung, “Algorithms for non-negative matrix factorization,” in *NIPS*, pp. 556–562, 2000.
- [25] W. Matusik, H. Pfister, M. Brand, and L. McMillan, “A data-driven reflectance model,” *ACM Trans. Graph.*, vol. 22, pp. 759–769, July 2003.
- [26] H. W. Jensen and J. Buhler, “A rapid hierarchical rendering technique for translucent materials,” *ACM Trans. Graph.*, vol. 21, pp. 576–581, July 2002.
- [27] R. Wang, J. Tran, and D. Luebke, “All-frequency interactive relighting of translucent objects with single and multiple scattering,” *ACM Trans. Graph.*, vol. 24, pp. 1202–1207, July 2005.